高速电弧喷涂枪结构优化的试验

陈永雄, 朱子新, 刘 燕, 徐滨士
(装甲兵工程学院 装备再制造技术国防科技重点实验室, 北京 100072)

陈永雄

摘 要: 试验优化了一种高速电弧喷涂枪的结构。用 SprayWatch 2i热喷涂监测系统测试了喷枪的雾化熔滴速度, 并研究了 Al涂层和 3Cr13涂层的组织和性能。结果表明, 丝材和导电嘴的存在, 严重扰动了雾化气流流态, 两丝夹角和丝交点离喷管出口距离也显著影响了喷管气流场的分布特征; 改进设计喷枪的雾化熔滴速度显著提高, 其 3Cr13雾化熔滴的最高速度达到 210 m/s, 涂层组织和力学性能也得到改善, 喷涂 Al涂层和 3Cr13涂层时, 结合强度分别提高了 55%和 39%, 硬度值也分别增加了 26%和 9%, 涂层的显微组织更均匀致密, 孔隙率更低。

关键词: 高速电弧喷涂枪; 涂层; 性能; 结构优化
中图分类号: TG174.442 文献标识码: A 文章编号: 0253-360X(2006)03-25-04

0 序 言

近年来, 电弧喷涂技术在热喷涂领域中占有越来越重要的位置。随着电弧喷涂设备的发展, 其涂层性能也有很大程度的提高。高速射流电弧喷涂技术(HVAS)系利用新型拉伐尔喷管设计, 采用高压气流或燃料燃烧产生的高速射流作雾化气流, 可加速熔滴的脱离, 使熔滴的加速度显著增加并提高电弧的稳定性[1,2]。在高速电弧喷涂技术中, 其关键设备是高速电弧喷涂枪, 学者们就如何提高喷枪的雾化质量已作了大量的工作[3~9]。由全军装备维修表面工程研究中心研制的 HAS-01型高速电弧喷涂枪喷涂 φ2 mm 丝材时, 涂层性能较普通喷枪有很大的提高。

为适应大规模工业生产的需要, 进一步提高喷涂的效率, 现在越来越倾向于喷涂 φ3mm、φ4mm甚至更大直径的丝材, 这就为高速电弧喷涂枪的发展提出了更高的要求。作者的研究就是从这一需求出发, 在原来主要喷涂 φ2 mm 丝材的 HAS-01型高速电弧喷涂枪的基础上, 研究出喷涂 φ3 mm 丝材时, 也能具备良好性能的高速电弧喷涂枪。

1 高速电弧喷涂枪的优化设计和测试方法

HAS-01型高速电弧喷涂枪的结构简图见图 1。在 HAS-01型喷枪结构的基础上, 考虑到引弧点离喷管出口距离、两丝夹角、导电嘴形状以及机加工的实际情况, 设计四种喷枪结构进行优化。参数见表 1, 其中 1号为 HAS-01型喷枪的结构特征, 导电嘴形状 A代表原来型号, B代表改进型号, 即在原来型号的基础上, 将导电嘴的前端(图 1示虚线 L 处)加工成一定角度的斜面。

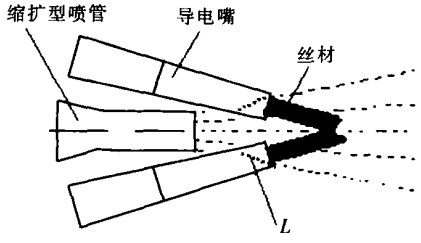

图 1 喷枪结构示意图
Fig. 1 Schematic configuration of HVAS gun

表 1 喷枪结构的设计参数
Table 1 Design parameter of spraying gun

喷枪编号	离出口距离 L/mm	丝材夹角 θ(°)	导电嘴型号
1	34	30	A
2	34	40	A
3	20	40	A
4	20	40	B

按上述方法加工出所需的零件、装配完成后, 依次进行喷涂试验, 采用 CMD-AS-3000型电弧喷

收稿日期: 2005-09-26
基金项目: 国家自然科学基金重大资助项目(50235030); 中国人民解放军总装备部维修改革项目(2003ZB06)

涂系统,选用 ϕ3 mm 的 Al和 3Cr13喷涂丝材,工艺参数见表 2.观察喷涂效果,并按国家标准 GB9796—88在 BMT-1试验机上分别测试涂层的拉伸结合强度,比较试验结果。确定喷涂效果最佳的喷枪并定型后,与 HAS-01型高速电弧喷涂枪展开性能对比试验,观察雾化熔滴的速度和粒度分布、分析涂层的显微组织特征、测试涂层的显微硬度和孔隙率。使用芬兰制造的 SprayWatch-2i型热喷涂监控系统测试喷涂过程中雾化熔滴的速度变化;用 QUANTA 200型扫描电子显微镜分析从水中收集到的粒子的分布特征;用金相显微镜观察涂层的显微组织;用ⅡMT-3型显微硬度计按国家标准 GB 9790—88测试涂层的显微硬度;采用图像分析仪参照国家标准 GB3365—82测试涂层的孔隙率。

表 2 喷涂工艺参数

Table 2 Operating parameters of HVAS

材料	电压 U/V	电流 I/A	喷涂距离 L/mm	空气压力 p_0/MPa
Al	30	140	250	0.6
3Cr13	34	180	250	0.6

2 试验结果及分析

2.1 高速电弧喷涂枪优化结果分析

结合强度是反映涂层综合质量的重要因素之一,表 3、4示出了四种结构喷枪所获得涂层的结合强度。从表中可以看出,喷涂 Al和 3Cr13丝时,第 4号喷枪对应的结合强度都较其它 3种喷枪要好,喷涂 Al时,其结合强度比 1号喷枪(HAS-01型)所对应的结合强度提高了 55%,喷涂 3Cr13时,结合强度提高了 39%。而且,从外观质量来看,喷涂时,4号喷枪喷出的焰流细长集中,获得的涂层表面明显均匀细密。图 2示出了 4号喷枪和 HAS-01型喷枪所获得的焰流特征,从图中可以看出,HAS-01型喷枪的焰流张角为 25°±1°,而 4号喷枪的张角缩小到 12°±1°,在 150~250 mm 这一喷涂距离内,相对 HAS-01型喷枪,4号喷枪雾化熔滴的分布更为集中,而且不再存在焰流的分叉现象,这在 HAS-01型喷枪上却非常明显。

可以看出,两丝夹角和引弧点离喷管出口距离这两个因素显著影响了喷管气流场的特征,并且由于丝材和导电嘴的存在,也严重扰动了气流流态。不同的引弧点位置、丝材夹角以及导电嘴形状设计,会使气体的动力学特征发生改变。缩短引弧点与喷管出口间的距离可以充分利用雾化气流出口后的动能,从而有效增加雾化熔滴的速度;增大两丝夹角可以缩短喷管出口与引弧点间的距离并减小丝材和导电嘴对雾化气流的影响,但过大的夹角会产生强激波而造成能量的急剧损失。因此,很有必要优化引弧点与喷管出口距离和两丝夹角这两个因素。而且,喷管与导电嘴合理设计也能改善喷涂的雾化效果,本研究提出的改进型导电嘴系在常规导电嘴前端加工一定角度的斜面,这样可以使气流得到二次收缩并加剧了丝材尖端涡流团的变化,从而减小了焰流的张角,充分雾化了熔融金属。通过这次试验,综合评价后,确定第 4种结构为最优设计,并将其定型为 HAS-02型高速电弧喷涂枪。

表 3 Al涂层的抗拉强度(MPa)

Table 3 Bonding strength of Al coating

	测试值				平均值
1	18.4	14.0	16.0	15.6	16.0
2	16.0	18.6	17.3	17.6	17.4
3	17.6	21.6	18.6	19.4	19.3
4	20.1	27.0	27.5	24.7	24.8

表 4 3Cr13涂层的抗拉强度(MPa)

Table 4 Bonding strength of 3Cr13 coating

	测试值				平均值
1	24.6	26.1	24.3	22.1	24.3
2	21.6	23.4	24.6	23.5	23.3
3	23.5	28.1	28.7	26.0	26.6
4	32.1	36.9	32.5	33.9	33.8

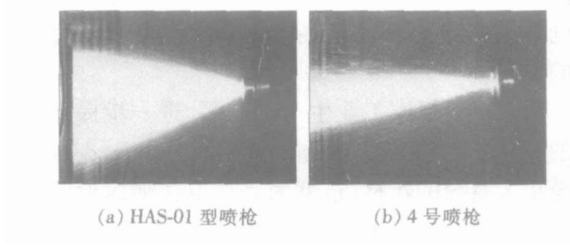

图 2 HAS-01型喷枪和 4号喷枪的射流特征

Fig. 2 Photographs of jet for HAS-01 gun and modified gun

2.2 雾化熔滴特征分析

图 3为两种喷枪在喷涂 ϕ3mm 3Cr13时雾化熔滴平均速度沿枪口的轴向分布情况。可以看出,HAS-02型喷枪熔滴自引弧点处喷射出来后,不断加速,到距引弧点 170 mm 时速度达到最大,为 174 m/s ±47.3 m/s,并且在 170~270 mm 这一区域内,熔滴速度也在这一较高值之间波动,这恰好是正常的喷

涂区域,而 HAS－01型喷枪在距引弧点 40 mm处雾化熔滴的平均速度为 117. 3 m /s并且呈线性下降趋势,在 150 mm 处下降至 93. 1 m /s远远低于 HAS－02型喷枪在同一区域内熔滴的速度。同时,通过比较两者所得粒子的粒度可以发现(图 4), HAS－01型枪喷涂时所得粒子的平均粒度为 47. 3 μm, HAS－02型枪所得粒子的平均粒度为 30. 2 μm,前者约为后者的 1. 6倍,且后者的粒径比较均匀。这一数值也验证了前面的优化过程得出的结论,优化丝材夹角和引弧点与喷管出口间的距离,使雾化气流动能得到最大限度的利用,并且创造性设计的新型导电嘴,有效的改善了雾化气流的流态,使高速射流更加集中。综合作用的结果,使熔滴速度得到提高,雾化更加细密均匀。

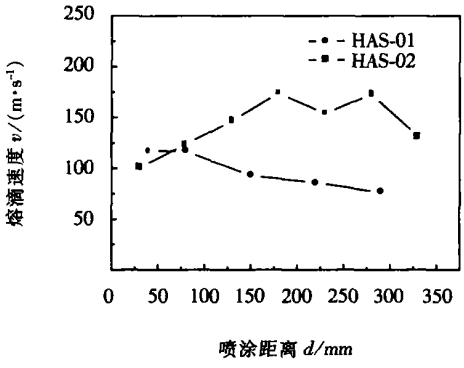

图 3　雾化熔滴速度的轴向分布

Fig. 3　Atomizing droplet velocity in axial direction

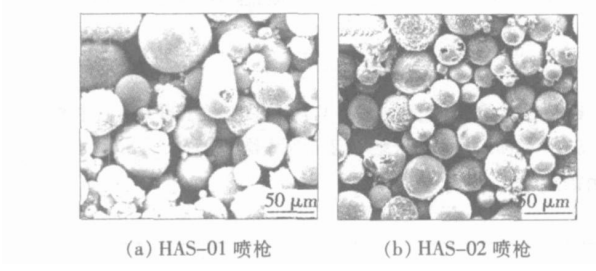

图 4　HAS－01喷枪和 HAS－02喷枪喷涂粒子 SEM形貌

Fig. 4　SEM micrographs of collected particles for HAS－01 gun and HAS－02 gun

2. 3　涂层的组织与性能分析

2. 3. 1　显微硬度分析

表 5为两种喷枪所得 Al涂层和 3Cr13涂层的显微硬度值。喷涂 Al时, HAS－02型喷枪所得涂层的平均硬度为 53. 7 HV,比 HAS－01型喷枪的值提高了 26%;喷涂 3Cr13时, HAS－02型喷枪获得涂层的平均硬度值为 445. 5 HV,比 HAS－01型提高了 9%。

表 5　涂层的显微硬度

Table 5　Coating Microhardness

材料	喷涂枪	平均显微硬度(HV)
Al	HAS－01	42. 6
	HAS－02	53. 7
3Cr13	HAS－01	407. 5
	HAS－02	445. 5

涂层的硬度主要取决于雾化颗粒的冷作硬化程度、氧化物的含量。一方面,因雾化颗粒飞行速度提高,在空气中停留时间短,合金元素的氧化损失较轻,冷作硬化程度提高;另一方面,雾化颗粒变细,比表面积增大,氧化程度增大,涂层氧化物含量升高。综合作用的结果使涂层的硬度升高。

2. 3. 2　显微组织分析

图 5为分别用 HAS－01型喷枪和 HAS－02型喷枪制备 Al涂层和 3Cr13涂层的组织形貌照片,可以看出, HAS-02型喷枪制备的涂层组织致密,层与层之间的距离明显缩小,孔隙的大小和数量也有所降低,涂层与基体结合良好。

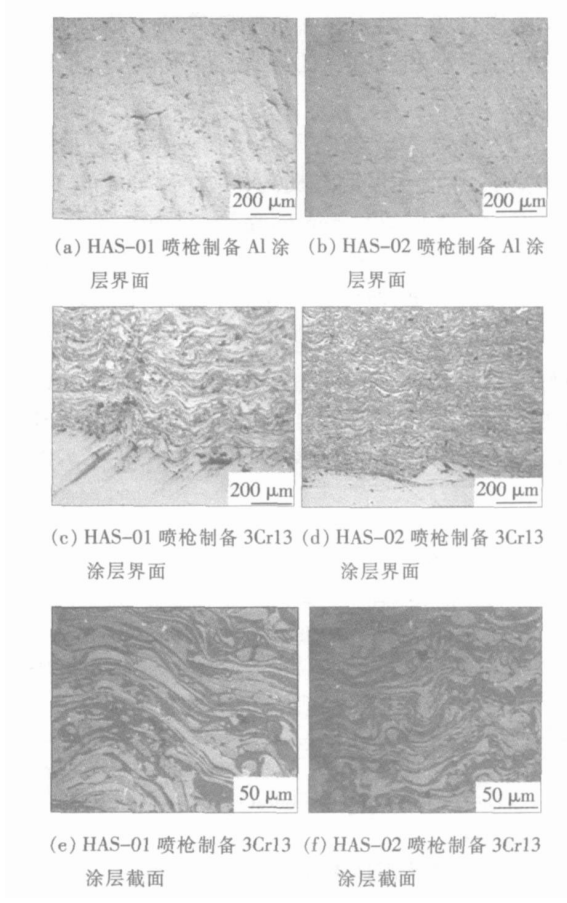

图 5　两种喷枪制备涂层的组织形貌特征

Fig. 5　Coating microstructures prepared by two different HVAS guns

表 6为两种喷枪制备 Al涂层和 3Cr13涂层的孔隙率结果。可以看出, HAS－02型喷枪制备的 Al涂层和 3Cr13涂层的孔隙率分别比 HAS－01型喷枪降低了 44%和 60%。这说明 HAS－02型喷枪制备的涂层,雾化粒子更细,粒子撞击基体时的速度更高,扁平化变形程度更大,涂层与基体之间以及层与层之间的结合良好,进而使涂层的组织更加致密,孔隙率更低。

表 6 涂层的孔隙率

Table 6 Porocity of coatings

材料	喷涂枪	孔隙率(%)
Al	HAS－01	2.45
	HAS－02	1.37
3Cr13	HAS－01	2.97
	HAS－02	1.18

3 结 论

(1)高速电弧喷涂枪两丝夹角和引弧点离喷管出口距离这两个因素显著影响喷管的气流场特征,并且由于丝材和导电嘴的存在,也严重扰动了气流流态。

(2) HAS－02型高速电弧喷涂枪的雾化射流更加集中,熔滴速度明显提高,喷涂 φ3 mm的 3Cr13丝材时,在 150～270 mm的喷涂范围内,雾化熔滴的最大速度高达 210 m/s,而且也解决了原有喷枪雾化射流的分叉现象,保证了良好的喷涂效果。

(3) HAS－02型高速电弧喷涂枪的涂层具有更好的力学性能,其 Al涂层的结合强度是 HAS－01型喷枪的 1.55倍, 3Cr13涂层的结合强度是 HAS－01型喷枪的 1.39倍,涂层的硬度值也有一定程度的提高,涂层力学性能提高的关键因素是雾化熔滴飞行速度的提高和均匀雾化。

(4) HAS－02型高速电弧喷涂枪涂层显微组织更加致密,与基体结合良好,孔隙率更低。

参考文献:

[1] 徐滨士, 梁秀兵, 马世宁, 等. 新型高速电弧喷涂枪的开发研究[J]. 中国表面工程, 1998, 11(3): 16－19.

[2] Xu Binshi. High velocity arc spray and its prospects[A]. 2000 ASM international material conference proceeding[C]. St. Louis, USA, 2000.

[3] 朱子新, 梁秀兵, 徐滨士, 等. 高速电弧喷涂熔滴速度的数值模拟及试验[J]. 焊接学报, 2002, 23(1): 5－8.

[4] Jinlin Wen, Songqing Wen, Weisheng Geng, *et al*. Supersonic arc spraying process[A]. Proceedings of the 14th international thermal spray conference[C]. Kobe, Japan, 1995.

[5] Lester T P, fitzsimons B. New methods, specifications and standards in offshore corrosion protection[A]. Proceedings of the 14th international thermal spray conference[C]. Kobe, Japan, 1995.

[6] Nakhlen Hussary. Investigations into the wire arc spraying process[D]. University of Minnesota, USA, 2003.

[7] Rogers F S. Benefits and technology developed to arc spray 3/16 inch(4.8 mm) diameter wires used for corrosion protection of steel[A]. Proceedings of the 16th international thermal spray conference[C]. Montreal, Canada, 2001.

[8] Gedzevicius, Bolot R, Liao H, *et al*. Application of CFD for wire－arc nozzle geometry improvement[A]. 2003 ASM international material conference proceeding[C]. Ohio, USA, 2003.

[9] Zhu Y L, Liao H L, Coddet C, *et al*. Characterization via image analysis of cross over trajectories and inhomogeneity in twin wire arc spraying[J]. Surface and Coatings Technology, 2003, 162(2): 301－308.

作者简介:陈永雄,男, 1978年 7月出生,硕士研究生。主要从事高速电弧喷涂技术的研究,发表论文 3篇。

Email: famon1599@163.com

[上接第 20页]

iors of fully-penetrated gas tungsten arc weld pool with surface deformation[J]. Proceedings of the Institution of Mechanical Engineers, Part B: Journal of Engineering Manufacture, 2005, 219(1): 99－110.

[12] Choi M, Greif R. A study of heat transfer during welding with applications to pure metals or alloys and low or high boiling temperature materials[J]. Numerical Heat Transfer, 1987, 11(4): 477－489.

[13] 武传松. 焊接热过程数值分析[M]. 哈尔滨: 哈尔滨工业大学出版社, 1990.

[14] Goldak J, Chakravarti A, Bibby M. A new finite element model for welding heat sources[J]. Metallurgical Transaction B, 1984, 15(6): 299－305.

作者简介:赵 明,女, 1973年 4月出生,博士研究生。主要研究方向为焊接过程数值模拟。共发表论文 2篇。

Email: meg10512001@yahoo.com.cn

versity, Jinan 250061, China). p17 – 20, 28

Abstract: It has been found that when the Gaussian or Double-elliptic mode of heat flux distribution was employed in numerical simulation of GTAW (gas tungsten arc welding) welding pool behaviors, there was marked difference between the predicted and practical pool geometry at the rear of weld pool. The reason why such difference exists was analyzed, and three principles guiding how to determine the calculating zone of heat source on the work piece were put forward in designing the numerical simulation program. Through appropriate selecting the calculating zone radius of welding arc on the work piece and making it matched with the distribution parameters of Double-elliptic mode of heat flux, the trailing problem of weld pool rear in previous models had been successfully solved, and the numerical simulation precision had been greatly improved for GTAW weld pool geometry.

Key words: weld pool geometry; rear trailing of weld pool; distribution mode of heat source; numerical simulation; gas tungsten arc welding

Technology characteristics of stainless steel plasma arc gas tungsten arc double sided arc welding process DONG Hong-gang[1,2], GAO Hong-ming[2], WU Lin[2], LIU Li-ming[1] (1. Laboratory of Special Processing of Raw Material, Department of Materials Engineering, Dalian University of Technology, Dalian 116024, China; 2. National Key Laboratory of Advanced Welding Production Technology, Harbin Institute of Technology, Harbin 150001, China). p21 – 24

Abstract: This paper analyzes the technology characteristics of stainless steel plasma arc gas tungsten arc double-sided arc welding process which could increase penetration and reduce distortion, then this process is applicable to weld the thick plate. After the keyhole was established, the arcs during the double – sided arc welding are apparently constricted to some extent, and the arc voltage between the two welding torches descends, which can economize on energy. Because the arc heats the workpiece within the weld pool after penetrating, the arc thermal efficiency was improved. The surface tension, arc blow force and electromagnetic force work positive to improve the penetration, and the buoyancy can increase the width in the middle of weld pool.

Key words: double sided arc welding; keyhole; plasma arc

Configuration optimization of a high velocity arc spraying gun CHEN Yong-xiong, ZHU Zi-xin, LIU Yan, XU Bin-shi (National Key Laboratory for Remanufacturing, Academy of Armored Forces Engineering, Beijing 100072, China). p25 – 28

Abstract: The configuration of high velocity arc spraying (HVAS) gun was optimized, the atomized particle velocity of the HVAS gun was measured by the Spraywatch-2i monitor system. A comparative study was carried out to investigate the microstructure and properties of the coatings produced by the original gun and the modified gun using 3mm diameter Al and 3Cr13 wires. The results indicated that angle and the distance from the nozzle to the meeting point of the two wires may have a strong influence on the characteristics of the in-flight droplets and the coatings; and the existing of wires and wire guides exited in the mater jets also affected the distribution of the air flow field. Using the optimized gun, the atomized particle velocity is increased remarkably, and the coating microstructure and properties are improved relatively. The adhesion strength of the Al and 3Cr13 coatings deposited by the modified gun increased 55% and 39% respectively, and the hardness increased 26% and 9% respectively. The microstructure of the coatings was more dense and homogenous, and the porosity also decreased a little. When spraying 3Cr13, the highest particle velocity is about 210 m/s in the range of 170 – 270 mm from the nozzle to the meeting point of the two wires.

Key words: high velocity arc spraying gun; configuration optimize; coating; property

Detect and analysis of molten droplet in short circuit arc welding based on high-speed charge coupled device camera ZHU Zhi-ming, WU Wen-kai, CHEN Qiang (Tsinghua University, Beijing 100084, China). p29 – 33

Abstract: An experimental system to photograph molten droplet images by using a high-speed charge coupled device camera and to record welding current and arc voltage in phase was established. After the definition of molten droplet size in short circuit transfer mode was given and the analysis system for molten droplet size and arc signals based on MATLAB platform was introduced, the characteristic of molten droplet size in short circuit CO_2 arc welding using the power supply with constant voltage output, the relationship between the molten droplet size and the welding process behavior were investigated. The experimental results show that the molten droplet size presents normal distribution between 1 and 2 times of wire electrode diameter. The excessive large or small size in molten droplet are all unfavorable to the stability of welding process in short circuit transfer mode. According to the formation and transfer course of molten droplet, the main influence factors to the molten droplet size are analyzed and the approaches to control the droplet size are proposed. Namely, the random characteristic of the residual liquid metal quantity at the end of wire electrode after the completion of short circuit transfer and the arc energy induces the uncertainty of molten droplet size; (making effective control on them will increase the accordance of molten droplet size and short circuit transfer procedure, and improve the process behavior and welding quality of short circuit CO_2 arc welding further.)

Key words: high-speed charge coupled device camera; droplet size; short circuit transfer; random characteristic

Fatigue design curve of tubular joints treated by ultrasonic peening WANG Dong-po, WANG Ting, HUO Li-xing, ZHANG Yu-feng (College of Material Science and Engineering, Tianjin University, Tianjin 300072,